Effects of Cr and Mn dopants on the density of states of superconducting niobium and vanadium

D. S. Buchanan,* A. Roy, D. M. Ginsberg, and J. E. Cunningham
Department of Physics and Materials Research Laboratory, University of Illinois at Urbana—Champaign, Urbana, Illinois 61801
(Received 6 September 1983)

We have made proximity-effect electron-tunneling measurements on films of Nb and V, pure and doped with Cr and Mn. In contrast to predictions of the theory of Shiba and Rusinov for magnetically doped superconductors, we see no well-defined bands of states below the superconducting gap edge.

I. INTRODUCTION

With the development of proximity-effect tunneling by Wolf *et al.* many superconducting materials became reliably accessible to the technique of electron tunneling for the first time. Wolf *et al.* used the technique to investigate transition elements and their alloys, such as Nb (Ref. 1), V (Ref. 2), and $Nb_{1-x}Zr_x$.[3] We have used it to look at Nb and V doped with Cr and Mn. Whereas the former studies were focused on the electron-phonon interaction, we were interested in looking at the electron—magnetic-dopant interaction using Mn and Cr as our possibly magnetic dopants. We present here tunneling data for these systems and compare our results with the predictions of the theory of Shiba[4] and Rusinov.[5] Their theory gives the same low-temperature density of states as that of Müller-Hartmann and Zittartz, at least for the case where only s-wave scattering is considered; this theory has been reviewed by Müller-Hartmann.[6]

The theory of Shiba and Rusinov predicts that bands of localized states will appear in the gap region of the density of states (DOS) of a superconductor as a result of the exchange interaction between magnetic dopant atoms and the conduction electrons.[7] Each band will be characterized by a parameter ϵ_l, where l is the orbital angular momentum. The band will appear at an energy $\epsilon_l\Delta$, where Δ is the superconducting order parameter. The area of each band will be proportional to the doping concentration. As we will see, Cr and Mn do not produce well-defined bands in Nb or V, however, and we will list some possible explanations for this fact.

Nb and V have, in the past, proved to be very difficult to study by conventional electron-tunneling spectroscopy. Early attempts on Nb (Ref. 8) gave rise to strange results. Later studies[9] revealed that the oxidation of Nb to form the insulating barrier of Nb_2O_5 is accompanied by the formation of an underlying layer composed of NbO, a superconductor ($T_c=1.4$ K),[10] and NbO_2, a semiconductor.[10] This layer complicates the interpretation of the tunneling data. The first quantitatively successful tunneling on Nb was done by Wolf *et al.*[1] They prevented the formation of a layer of oxides by covering a clean surface of Nb with a thin layer of Al which was then oxidized. They could control the Al thickness, and they used a quantitative theory, developed by Arnold,[11] to treat this proximity sandwich. If the Al layer left after oxidation is sufficiently thin, it can be ignored in analyzing the data. For V the situation is similar. VO is a semimetal,[10] and VO_2 is a semiconductor.[10] Zasadzinski *et al.*[3] successfully extended the proximity technique to V, so we use it on our V samples also.

II. PREPARATION OF THE Nb SAMPLES

Our samples were made[12] in a molecular-beam epitaxy (MBE) facility which had been assembled specifically for working with metals. To make our samples we evaporated the host material from an electron-beam gun while evaporating the dopant from an oven. The Al was subsequently evaporated from another oven source. All depositions were begun and ended by moving shutters. The substrates were glass microscope slides, cleaned successively with detergent, acetone, and ethanol. We used marz grade Nb from Material Research Corporation (99.99% pure, except for a Ta concentration of 180 ppm). The Cr was 99.999%-pure material from Johnson, Matthey and Co., Ltd., and the Mn was 99.99%-pure metal from A.D. Mackay, Inc.

The substrates were held at 200 °C during the depositions because Nb films deposited onto the substrates held at room temperature had a tendency to flake off. Because Cr and Mn are not soluble in Nb, we did not want to use a higher temperature; the dopants might have precipitated out of the Nb. In bulk Nb the diffusion constant (Ref. 13), D, of Cr is approximately $(0.3\ \text{cm}^2/\text{sec})\exp(-Q/RT)$, where $Q=83.5$ kcal/mol. For $T=473$ K, $D=8\times10^{-40}$ cm^2/sec, so diffusion through $l=10$ Å requires a typical time of $t=l^2/D$, approximately 4×10^{17} yr. Surface diffusion would have a value of Q roughly one-half of the bulk value, and a typical time for diffusion through 10 Å would be 7.5 d.

A reliable and accurate calibration of the source, a crucial factor in the manufacture of dilute alloy films, was accomplished in the following manner. The MBE system contained a quadrupole mass spectrometer (MS) which was monitored by a computer. The computer controlled the emission current of the electron-beam gun, providing feedback control for it. The rate of deposition of the dopant atoms was controlled by regulating the oven temperature. We calibrated the MS by depositing material at a constant MS reading for a measured length of time and then determining the thickness of the resulting film by multiple beam interferometry.[14] A problem that arose

TABLE I. Comparison of the concentration determined from the deposition and as determined by SIMS.

Sample no.	Nominal concentration (atomic ppm)	Measured (SIMS) concentration (atomic ppm)	Dopant
A	0	0	
B	0	0	
C	300	109	Cr
D	300	340	Mn
E	600	221	Cr
F	600	355	Mn

with this procedure was that the MS calibration would remain stable only for periods on the order of a week. To expedite the frequent recalibration of the MS we installed a quartz-crystal monitor. We measured the change of crystal frequency with film thickness, and obtained a calibration which was stable. Using the crystal, we recalibrated the MS immediately before each run. The low deposition rate of the dopant materials introduced another problem in the calibration procedure. Because the Nb deposition was limited to rates on the order of 2 Å/sec, and because the doping levels were on the order of 300—600 ppm, we had to deposit the dopant atoms at rates of only $6-12\times10^{-4}$ Å/sec. (All concentrations in this paper are given in atomic parts per million.) We had to do the calibration of the dopants at much higher deposition rates than we used during the sample depositions. To determine the deposition rates of the dopants during the sample depositions, we depended on the linearity of the MS's control unit. The validity of this approach was tested by comparing the nominal concentrations of dopants in our samples with those determined by secondary-ion mass spectrometry (SIMS) (Table I). The Al source was calibrated in the same way as the dopant source except that the rates used for the calibration and the rates used for the deposition were both on the order of 1.0 Å/sec.

The flux of atoms coming from the electron-beam source was found to have a spatial variation, and the calibration remained valid only while the spatial variation remained constant. To keep it constant we had to have the same amount of material in the source at the beginning of each run and we also had to have the high voltage of the electron-beam gun set to the same value for both the calibration run and the sample deposition.

The samples were deposited in pressures between 5×10^{-9} and 1×10^{-8} Torr. The Nb was deposited at rates of 1.5—2.0 Å/sec and the dopants at rates calculated to yield the desired doping concentration. The samples were made with a nominal thickness of 3000 Å, so the deposition times were between 25 and 35 min. Toward the end of the sample deposition the Al source was brought up to operating temperature. As soon as the sample deposition was complete the substrate heater was turned off, a shutter was opened, and the Al layer was immediately applied. Approximately 50 Å of Al was deposited, as measured by the crystal monitor. The changeover from the sample deposition to the Al deposition took 15—30 sec.

After the substrate had cooled to room temperature we removed it from the MBE system and allowed the sample to oxidize in room air for 2—3 h. We then placed it in another evaporator where we deposited 1500 Å of SiO to mask off the edges of the film. We then deposited 700 Å of Al in three strips across the film to form the counterelectrodes of our junctions. In the next section we will discuss the results obtained for our four successful sets of junctions, two of pure Nb, one doped with 300 ppm Cr, and one doped with 300 ppm Mn.

III. RESULTS FOR Nb

A. General properties of the Nb samples

In addition to our tunneling samples we made 2.5-μm-thick film in which one of us made susceptibility measurements.[15] These measurements showed that both Cr and Mn retain a magnetic moment in Nb.

Once we had good samples we measured the superconducting properties, including the superconductor-insulator-superconductor (SIS) I-V tunneling characteristic of each junction and its derivative, dI/dV, at both low- and high-voltage biases. We also measured the lattice parameter by x-ray diffraction, and determined the resistivity ratio of each film. The resistivity ratio is defined as the ratio of the resistance of the film at room temperature to its resistance at a temperature just above T_c. A summary of these parameters is given in Table II. The value of T_c for each film was measured resistively by using a four-terminal dc technique. The T_c of the Al counterelectrode was found by determining the temperature at which the thermal cusp in the I-V curve disappeared. This temperature could be located to ±2 mK.

The method of sample preparation left us with a fairly large uncertainty in the concentration of the dopant, so we obtained an independent measure of it by SIMS. A sam-

TABLE II. Superconducting properties, resistivity ratios, and lattice parameters for the Nb samples.

Sample no.	Nb T_c (K) ±0.01 K	Transition width (mK)	Nb Δ (meV) ±0.004 meV	Al T_c (K) ±0.01 K	Resistivity ratio ±1%	Lattice parameter (Å) ±0.001 Å
A	9.121	22	1.509	1.268	4.33	3.2937
B	9.266	31	1.506	1.250	11.66	3.2899
C	9.037	45	1.464	1.261	3.80	3.2937
D	9.120	30	1.479	1.294	3.41	3.2896
E	9.198	20	1.506	1.267	3.20	3.2837
F	9.245	25	1.523	1.381	5.86	3.2951

ple mass of around 65 μg ruled out other techniques. In order to obtain quantitative information, we used ion-implanted standards. The results are given in Table I. We could not measure the concentration to better than a factor of 2 because the measurement of the standards fluctuated by a factor of 2 from run to run. The SIMS work verified that there were no gross errors in the deposition procedure; from now on we will therefore use the nominal concentrations, derived from the deposition procedures. We believe that these are accurate to a factor of 2.

The measured resistivity ratio of each sample (Table II) gave us an indication of the crystal quality of our films. For Nb films deposited on sapphire substrates at high temperatures, resistivity ratios as high as 150 have been obtained;[16] x-ray studies done on those films showed them to be single-crystal samples. Our films, on the other hand, have resistivity ratios from 3.2 to 11.7. This may indicate a large degree of polycrystallinity in our samples.

We measured the lattice constants of our films using x-ray diffraction. Although we found a correlation between the lattice parameters and the T_c's of the pure Nb films, there was too much scatter in the data to enable us to use this correlation to determine the T_c depression caused by the doping.

On each sample we measured the derivative of the I-V characteristic at voltages between 4 and 45 meV. These are the voltages between which phonons of both the Nb and Al appear. In the data from our junctions the Nb phonons appeared at the correct voltages and with the correct strengths, but there was no indication of Al phonon structure at 38 meV, showing[17] that the Al proximity layer remaining after the oxidation of the Al overlayer was less than 10 Å thick. We therefore ignore the effects of the Al layer in the rest of our analysis.[1]

Our first good sample was sample A, a pure Nb film. Sample B was another pure Nb film, but its tunneling characteristics were considerably smeared out as we will show. (There were two good junctions on this sample. The third junction was shorted.) Sample C was Nb doped with 300 ppm Cr, and sample D was Nb doped with 300 ppm Mn. On each of these samples there were three junctions having the same characteristics. We made two samples with a doping level of 600 ppm: sample E with Cr, and sample F with Mn, but we had trouble with both of these samples. For sample E, there was poor thermal contact between that particular sample and the sample holder. Sample F showed a pathological behavior—a large number (approximately 10) of distinct structures in the gap re-

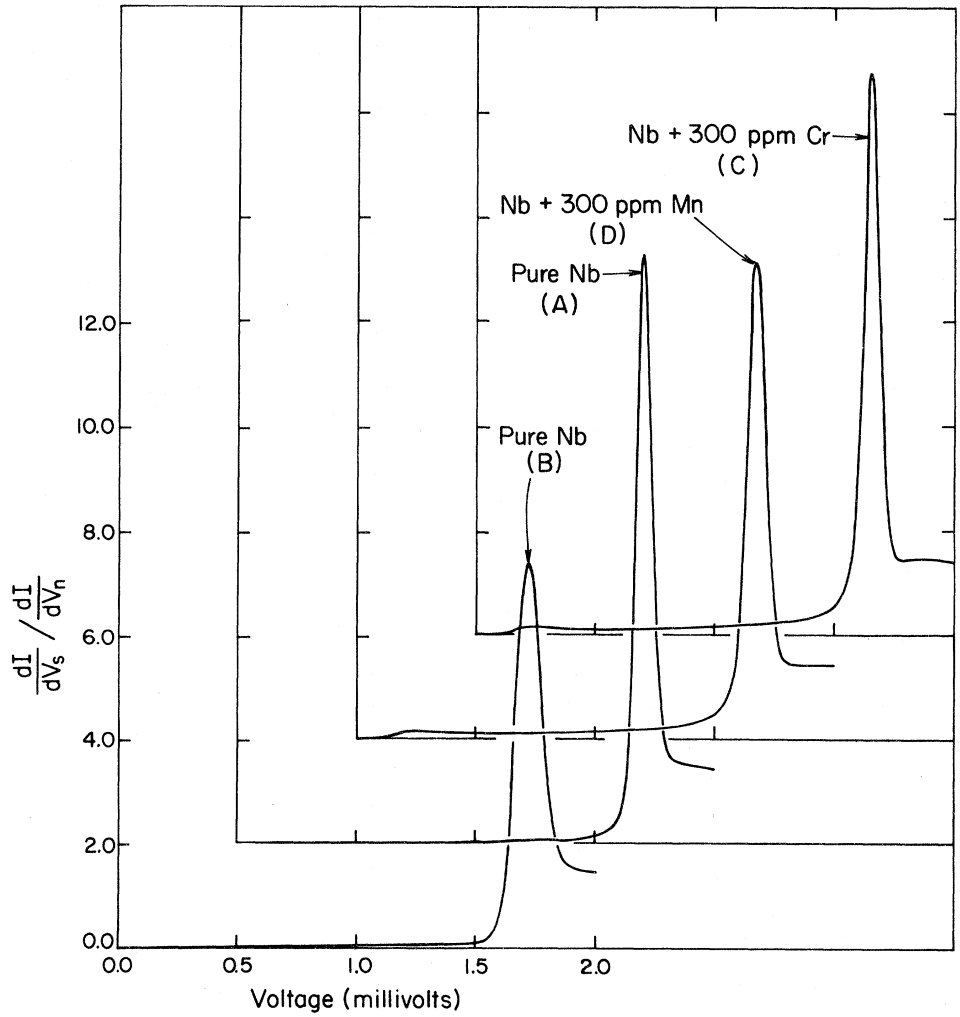

FIG. 1. Normalized dI/dV curves for our Nb samples. Each successive curve is shifted up by 2.0 and shifted to the right by 0.5 meV.

gion. Since we had seen this type of irreproducible behavior in a number of both pure and doped samples made before sample A we did not use the results from this sample. We will now look at samples A (pure), B (pure), C (300 ppm Cr), and D (300 ppm Mn).

B. Low-energy DOS

In Fig. 1 we show the normalized derivative curves for samples A, B, C, and D. The normalized derivative is defined as dI/dV in the superconducting state divided by dI/dV in the normal state. All low-energy data were taken between 0.37 and 0.39 K, using a harmonic detection technique. The ac excitation voltage for the harmonic detection was 20 μV peak to peak. The normal-state conductance was independent of voltage to less than 0.1%. In Fig. 2 we show the DOS curves calculated[12] from these data. It is obvious that there are no well-defined bands of states, but there are apparently many states at energies less than Δ for the doped samples C and D.

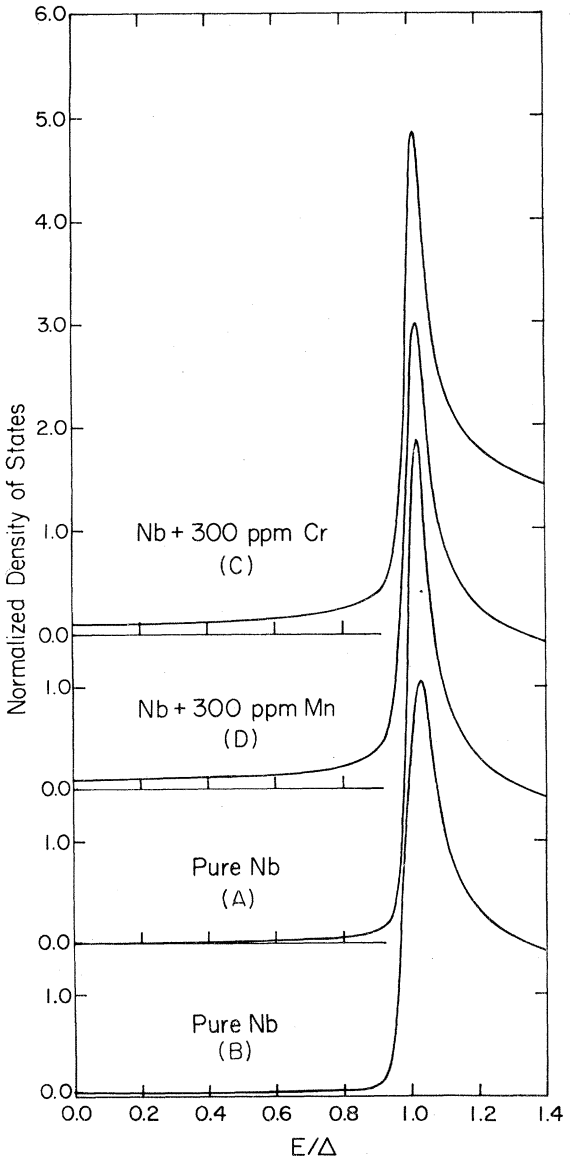

FIG. 2. DOS curves derived from our Nb data. Each successive curve is shifted up by 1.5.

Each DOS has a finite value near zero energy. The signature for this phenomenon is a rise in dI/dV from a small value (<0.01) at $V=0$ to a peak at low voltage (approximately 0.2 mV as seen in Fig. 1), indicating tunneling from the superconducting aluminum electrode into an essentially constant DOS as in a normal-insulator-superconductor (NIS) tunnel junction. At first glance the DOS near zero energy seems to increase with doping level. Unfortunately, when we looked at some of the pure samples previous to A and at samples E and F, we saw that this value varies independently of the doping level. This low-energy contribution to the DOS might be due to some NIS junction or junctions parallel with the SIS junction. It is possible to subtract off the effect of this type of junction. To do this, we take the value of the DOS at zero energy, D, and find a new DOS $N'(V)=[N(V)-D]/(1.0-D)$. We can see this by considering that the NIS junction contributes to the conductance of the junction in both the superconducting and normal states. The subtraction in the numerator accounts for the contribution in the superconducting state, and the subtraction in the denominator accounts for the contribution in the normal state. The resulting DOS curves are shown in Fig. 3 along with smeared BCS curves derived as explained below.

C. Peak heights of the dI/dV curves

The peak heights of the data, even for the pure samples, were less than the theoretical peak heights. We have done the following rough but reasonable calculation to try to account for this phenomenon, which we attribute to energy smearing.

We found that for the pure Nb we could get a reasonable match between predictions of the BCS theory[18] and our data by applying to the theoretical tunneling curve a simple Gaussian smearing of the type

$$f'(x_0)=A\int_{-\infty}^{\infty} dx\, f(x)\exp\left[-\left[\frac{x-x_0}{\sigma}\right]^2\right]. \quad (1)$$

We adjust σ to make the theoretical peak height match the observed peak height. This is shown in Fig. 4. From BCS we know that

$$\Delta=2\hbar\omega_D e^{-1/N_0V}. \quad (2)$$

In Nb the Fermi energy lies close to a very sharp peak in the DOS.[19] From the width of our observed x-ray diffraction lines, after accounting for the instrumental broadening by subtracting off the width of the calibration peak of a silicon-crystal standard, we obtain a statistical variation in the lattice parameter. This in turn gives rise to a variation in the local electronic density which moves the Fermi energy relative to a sharp peak in the DOS, changes the DOS at the Fermi energy, and therefore causes a variation in Δ. We are using the rigid-band approximation. To quantify the argument, we need both the DOS and slope of the DOS at the Fermi surface. We can get an estimate of these from Ref. 19. The magnitude of the slope is ap-

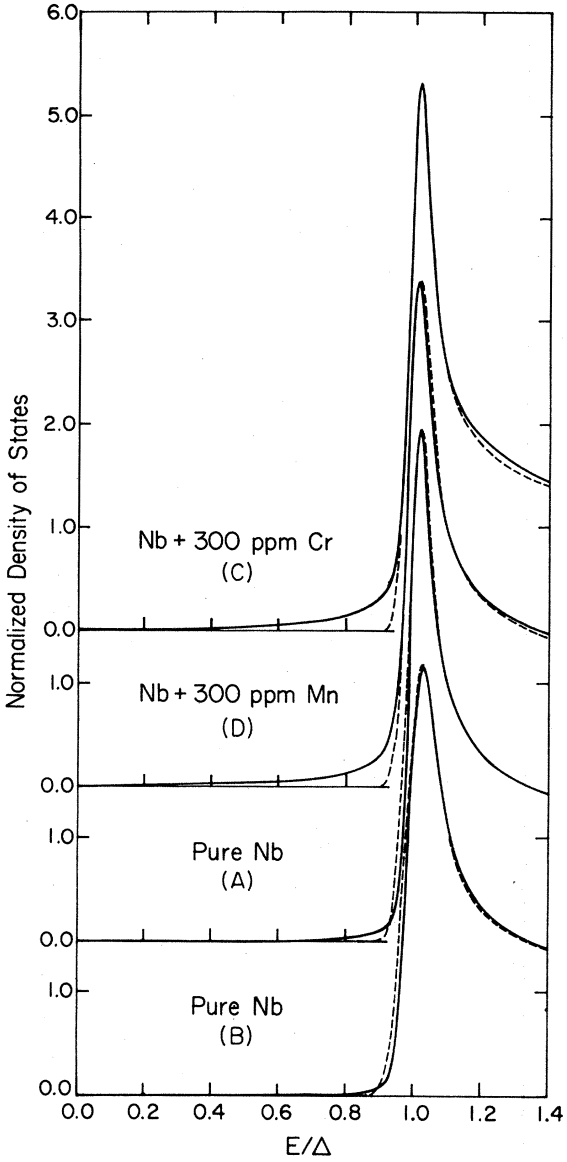

FIG. 3. Solid curves show the DOS for our Nb data after subtracting off the zero-bias DOS. The dashed curves show the smeared BCS DOS. Each successive curve is shifted up by 1.5.

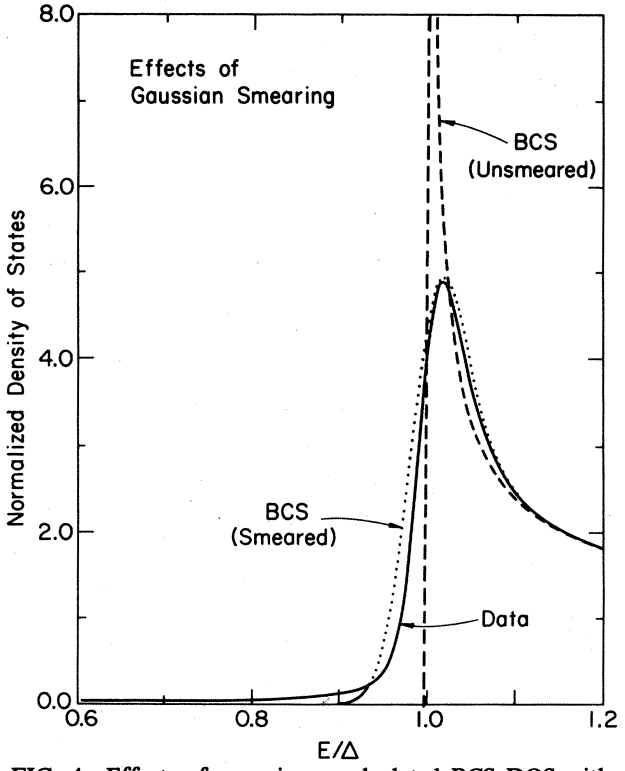

FIG. 4. Effects of smearing a calculated BCS DOS with a Gaussian. The smeared BCS curve corresponds to a smearing of $\sigma=0.0415\Delta$.

proximately 1.1×10^{47} states/cm^3 erg^2, and N_0 is 6.4×10^{34} states/cm^3 erg. Our x-ray linewidths are on the order of 0.3° at $2\theta=38.6°$. Using the BCS expression for Δ and relating the variation in the electron density to the change in DOS we can write

$$\frac{\delta\Delta}{\Delta}=\frac{\delta n_{\text{elec}}}{N_0^2}\ln\left[\frac{2\hbar\omega_D}{\Delta}\right]\frac{dN_0}{d\epsilon_f}\ . \tag{3}$$

We can use this to calculate the slope in the DOS, $dN_0/d\epsilon_f$, necessary to cause a 4% variation in Δ. We approximate $\hbar\omega_D$ by $0.75\Theta_D$, the average Debye phonon energy. We obtain a value of 1.0×10^{46} states/cm^3 erg^2. Nb has perhaps the largest slope in the DOS at the Fermi surface for any material measured by tunneling so far, and our tunneling measurements indicate the largest degree of smearing of the bands associated with the magnetic dopants.[20–25]

Two other groups have worked with Nb junctions of the type we use. Unfortunately there are enough differences between our work and theirs to make comparisons difficult. Rowell and co-workers[26,27] made Nb junctions with a thin Al overlayer, but they used a normal counterelectrode and took their data at $T\sim1.1$ K. They did not publish any derivative data in the gap regions of their junctions. Wolf *et al.*[1] used In as their counterelectrode, and they also took their data at $T\sim1.4$ K. They published one derivative curve in the gap region of one of their junctions. It showed a peak height of 9 in reduced conductance, and a width comparable to that of our pure junction's characteristics. Gap smearing has been seen in most, if not all, experiments on superconductor-insulator-superconductor tunneling, going all the way back to the classic work of Giaever, Hart, and Megerle on Pb.[28]

D. Absence of well-defined bands

If we look again at Fig. 3 we see that there are no well-defined bands of states below the energy gap. There does, however, appear to be a greater number of states there for the doped samples than for the pure samples. Figure 5 shows an enlarged picture of the gap region of Fig. 3. The increased area under the doped sample curves could be the result of the doping—a calculation[12] of the dopant concentration from this area yields a value close to 300 ppm for an assumed combination of *s*- and *p*-wave scattering for both the Cr- and Mn-doped samples. Although this is

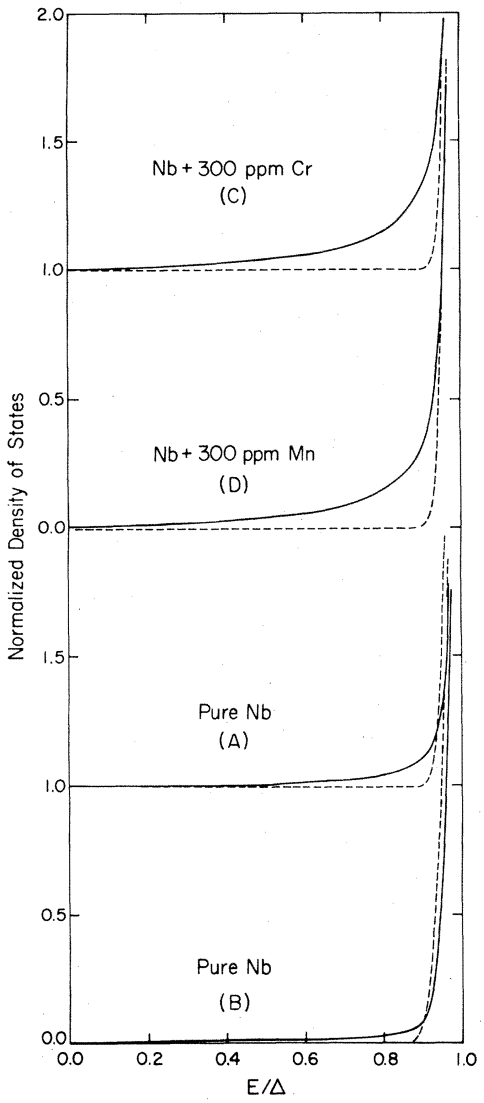

FIG. 5. Enlargement of the gap region of Fig. 2. Each successive curve is shifted up by 1.0.

suggestive, the increased area could also result from the mechanism causing the higher DOS at zero energy. The pure samples, as well as samples *E* and *F*, also showed extra area under the dI/dV-vs-V curve below Δ. This area, however, was not proportional to the dopant concentration. We conclude that the extra area seen in all the samples may be due to problems in the sample-making process. It has been clearly seen before in proximity-effect tunneling measurements on a bulk sample of a Nb-Zr alloy,[3] and may be related to gap smearing.

IV. PREPARATION OF THE V SAMPLES

The V samples were made in a manner which differed in the following ways from the preparation of the Nb samples. Because both Cr and Mn are soluble in V (Ref. 29) we did not have to restrict the temperature of the substrate. From previous work[16] done in the same MBE system, we knew that epitaxial V films could be grown on polished sapphire substrates if they were held at 800 °C. Our substrates were therefore held at that temperature in a molybdenum holder during the deposition of the V alloys. The V was marz grade V from the Materials Research Corporation (99.95% pure).

There are two other major differences between the Nb and V depositions. Because V has a higher vapor pressure, we could deposit the V at approximately 10 Å/sec. Also, because of the higher substrate temperature we found that we could not deposit the Al overlayer immediately after finishing the V deposition. We had to wait until the substrate temperature had dropped to 200 °C in order to get good junctions. This typically took 25 min. During that time all of the sources were turned off, and the pressure in the system was around 1×10^{-9} Torr.

V. RESULTS FOR V

We made susceptibility measurements[15] on V samples which were 2 μm thick. The interaction between the dopant atoms and the relatively large magnetic moments of the V atoms made it difficult to interpret the data. We believe, however, that there is evidence for the presence of localized moments on both Cr and Mn in V. We made six V samples for the tunneling experiment. Their characteristics are shown in Table III. All nominal concentrations are derived from the deposition procedure as described above. As with the Nb we made three junctions on each sample. On each V sample the three junctions showed the same tunneling characteristics.

Each of the V samples, except for sample *L*, had a very large zero-bias DOS; approximately 0.12—0.15 on a normalized scale; sample *L* had a zero-bias DOS of only 0.014. The gap edges of the tunneling characteristics were also very smeared out. Fitting them with a smeared BCS DOS required a σ of about 0.10Δ. X-ray data were also taken on the pure V sample. The x-ray peak was not significantly broader than that of the silicon standard so that the analysis applied to the Nb would not seem to apply to

TABLE III. Superconducting properties and resistivity ratios for the V samples.

Sample no.	V T_c (K) ±0.01 K	Transition width (mK)	V Δ (meV) ±0.004 meV	Al T_c(K) ±0.01 K	Resistivity ratio ±1%	Nominal concentration
G	5.338	9	0.790	1.351	51.9	0
H	5.255	11	0.784	1.307	30.8	200 ppm Cr
I	5.278	8	0.766	1.361	30.0	330 ppm Cr
J	5.227	12	0.767	1.341		590 ppm Cr
K	5.318	43	0.787	1.278	56.7	320 ppm Mn
L	5.203	7	0.809	1.386	21.7	350 ppm Mn

the V. It may be, however, that surface strains on the V due to the aluminum oxide would create variations in the local electron density near the surface. This would show up as a smearing of the gap in the tunneling curves because of the surface sensitivity of the tunneling probe. The Fermi energy in V also lies on the side of a sharp peak in the DOS.[30] Figure 6 shows plots of the DOS for the pure V sample and for sample L, which was doped with 350 ppm Mn. The zero-bias DOS was subtracted off before plotting the graphs, as described above. As we can see in the figure, sample L has no well-defined bands of impurity-associated states. This is true of the other doped samples as well except for sample J with 590 ppm Cr.

In the 590-ppm-Cr sample there seemed to be some states localized between the energies 0.5Δ and 0.9Δ. But even if we take this range by itself the area under the DOS curve corresponds only to 230 ppm for an assumed s-wave scattering (less for assumed p- or d-wave scattering). A structure one-half its size does not appear in the 390-ppm sample. We therefore do not believe that this structure is caused by the dopants. This junction was also different in that it had a very high normal-state resistance, 246 kΩ. The rest of our V junctions ranged from 31 to 763 Ω.

For V, Zasadzinski *et al.*[3] have also done proximity-effect tunneling. They used In as their counterelectrode and made their measurements at 1.4 K, giving approximately the same reduced temperature for their counterelectrode as we had for ours. They measured a peak height of 9, in normalized conductance. This is higher than for our junctions, for which the peak heights were between 4 and 5. There were two major differences between their technique and ours. Their V was in the form of a foil, and they were able to cool the V to −100 °C before depositing the Al overlayer. Unfortunately, we could not afford to wait until the V had cooled much below 200 °C before depositing the Al layer because of contamination at the background pressure; cooling to 200 °C took about 20 min. We can take the diffusion constant for V in Al from the work of Murarka *et al.*[31] and calculate how far the V diffuses into the Al while the substrate is cooling. The substrate starts at 200 °C when the Al is applied and cools to 150 °C about 5 min later. The diffusion constant is about an order of magnitude less at 150 °C than at 200 °C. We can therefore take the diffusion constant at 200 °C and the time of 5 min and calculate an upper bound for the distance the V has diffused into the Al, $l=(DT)^{1/2}$. This distance, l, is 16 Å. If we use the same procedure for Nb, using the diffusion constant measured by Tiwari and Sharma,[32] we get a distance of $l=75$ Å. Since our Nb junctions are of better quality than our V junctions, the diffusion of the V into the Al should not in itself make the V samples inferior to the Nb samples.

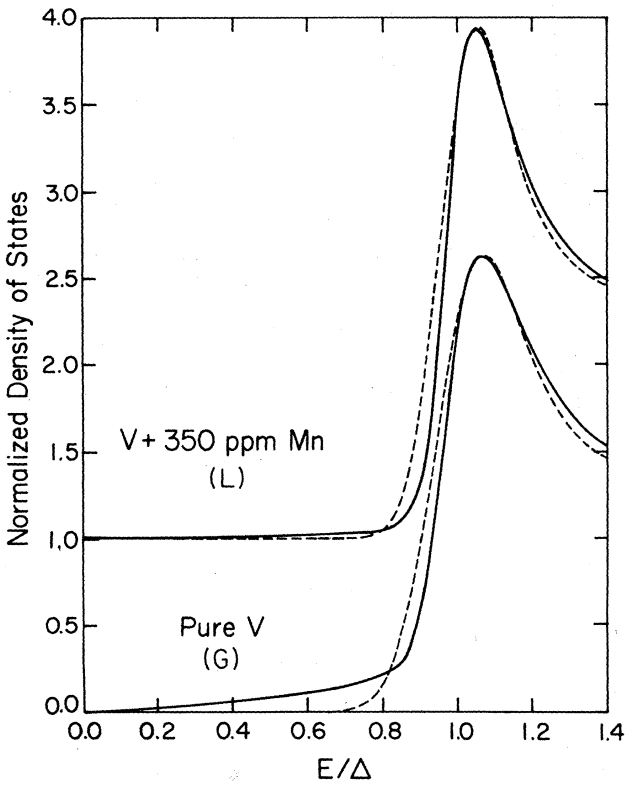

FIG. 6. Solid curves show the DOS for two of our V samples after subtracting off the zero-bias DOS. The dashed curves show the smeared BCS DOS. The top curve is shifted up by 1.0.

VI. CONCLUSIONS

Our tunneling data show that if Mn or Cr introduce states into the energy gap of Nb or V, these states must be much more smeared out than the theory of Shiba and Rusinov predicts. We believe that in Nb any band of states in the gap would be partially smeared out by a spatial variation in the Fermi energy caused by an inhomogeneity of the lattice constant. This variation would cause an inhomogeneity of the DOS at the Fermi energy because the Fermi level lies on the side of a steep peak in the DOS. Because all other measurements on magnetically doped superconductors also show smearing of the bands there are probably other mechanisms contributing to it. One questionable assumption we have made is that the dopants are all in the same atomic configuration. There are several different possible configurations which each dopant atom could assume,[33] and if the dopants occupy multiple configurations this would smear out the bands in the gap. Also, all of the theories assume that the spins of the dopants have infinite lifetimes. A finite lifetime of the spins[34] would smear out the bands of states.

The absence of well-defined bands of states associated with magnetic atoms in Nb and V contrasts with the presence of such states in Pb, In, and Zn.[22–25] Nb and V have shorter coherence lengths than these other metals, and have band structures which place the Fermi level near large peaks in the normal-state electronic DOS. We speculate that these features of Nb and V may not be properly included in the present theories of magnetically doped superconductors. One other possibility might be that the Mn and Cr are not magnetic near the sample surface. Because of the shorter coherence lengths of Nb and V, tunneling would only tell us of the near-surface region of the film.

ACKNOWLEDGMENTS

We thank Su Sing Chan for preparing the standards for the SIMS analysis and Judy Baker for doing the SIMS analysis. Data acquisition by three of us (D.S.B., A.R., and D.M.G.) was supported by the National Science Foundation under Grant No. NSF-DMR-82-03528. Sample preparation by two of us (D.S.B. and J.E.C.) was supported in part by the National Science Foundation under Grant No. NSF-DMR-80-20250.

---

*Present address: Los Alamos National Laboratory, Los Alamos, NM 87545.

[1]E. L. Wolf, J. Zasadzinski, J. W. Osmun, and G. B. Arnold, J. Low Temp. Phys. 40, 19 (1980).

[2]E. L. Wolf, R. J. Noer, and G. B. Arnold, J. Low Temp. Phys. 40, 419 (1980).

[3]J. Zasadzinski, D. M. Burnell, E. L. Wolf, and G. B. Arnold, Phys. Rev. B 25, 1622 (1982).

[4]H. Shiba, Prog. Theor. Phys. 40, 435 (1968).

[5]A. I. Rusinov, Zh. Eksp. Teor. Fiz. 56, 2047 (1969) [Sov. Phys.—JETP 29, 1101 (1969)].

[6]E. Muller-Hartmann, in *Magnetism,* edited by H. Suhl (Academic, New York, 1973), Vol. V, p. 353.

[7]D. M. Ginsberg, Phys. Rev. B 20, 960 (1979).

[8]L. Y. L. Shen, in *Superconductivity in d- and f-band Metals (Rochester),* Proceedings of the Conference on Superconductivity in *d*- and *f*-band Metals, edited by D. H. Douglass (AIP, New York, 1972), p. 31.

[9]I. Lindau and W. E. Spicer, J. Appl. Phys. 45, 3720 (1974).

[10]J. B. Goodenough, in *Progress in Solid State Chemistry,* edited by H. Reiss (Pergamon, Oxford, 1971), Vol. 5, p. 145.

[11]G. B. Arnold, Phys. Rev. B 18, 1076 (1978).

[12]D. S. Buchanan, Ph.D. thesis, University of Illinois at Urbana—Champaign, 1983 (unpublished).

[13]J. Pelleg, J. Met. 20, 53 (1968).

[14]S. Tolansky, *Multiple-Beam Interferometry of Surfaces and Films* (Oxford University Press, London, 1948).

[15]A. Roy, D. S. Buchanan, D. J. Holmgren, and D. M. Ginsberg (unpublished).

[16]S. M. Durbin, Ph.D. thesis, University of Illinois at Urbana—Champaign, 1983 (unpublished).

[17]E. L. Wolf (private communication).

[18]J. Bardeen, L. N. Cooper, and J. R. Schrieffer, Phys. Rev. 108, 1175 (1957).

[19]L. F. Mattheiss, in *Superconductivity in d- and f-band Metals (Rochester),* Proceedings of the Conference on Superconductivity in *d*- and *f*-band Metals, edited by D. H. Douglass (AIP, New York, 1972), p. 57.

[20]L. Dumoulin, E. Guyon, and P. Nedellec, Phys. Rev. B 16, 1086 (1977).

[21]W. Bauriedl, P. Ziemann, and W. Buckel, Phys. Rev. Lett. 47, 1163 (1981).

[22]J. K. Tsang and D. M. Ginsberg, Phys. Rev. B 21, 132 (1980).

[23]J. K. Tsang and D. M. Ginsberg, Phys. Rev. B 22, 4280 (1980).

[24]B. D. Terris and D. M. Ginsberg, Phys. Rev. B 25, 3132 (1982).

[25]B. D. Terris and D. M. Ginsberg, 29, 2503 (1984).

[26]J. M. Rowell, M. Gurvitch, and J. Geerk, Phys. Rev. B 24, 2278 (1981).

[27]J. Geerk, M. Gurvitch, D. B. McWhan, and J. M. Rowell, Physica (Netherlands), 109-110B&C, 1175 (1982).

[28]I. Giaever, H. R. Hart, and K. Megerle, Phys. Rev. 126, 941 (1962).

[29]W. G. Moffott, *Binary Phase Diagrams Handbook* (General Electric, New York, 1981).

[30]D. A. Papaconstantopoulos, J. R. Anderson, and J. W. McCaffrey, Phys. Rev. B 5, 1214 (1972).

[31]S. P. Murarka, M. S. Anand, and R. P. Agarwala, Acta Metall. 16, 69 (1968).

[32]G. P. Tiwari, and B. D. Sharma, Trans. Indian Inst. Met. 20, 83 (1967).

[33]A. B. Kunz and D. M. Ginsberg, Phys. Rev. B 22, 3165 (1980).

[34]M. B. Maple, in *Magnetism,* edited by H. Suhl (Academic, New York, 1973), Vol. V, p. 289.